ANL/GTRI/TM-14/6

Out-of-Pile Task 14.5.1: Impact of Mechanical Constraints on Peak Cladding Strain of U-10Mo Monolithic Plate

GTRI – Reactor Conversion Program
Out-of-Pile Testing and Codes
Task 14.5.1

Nuclear Engineering Division

About Argonne National Laboratory
Argonne is a U.S. Department of Energy laboratory managed by UChicago Argonne, LLC under contract DE-AC02-06CH11357. The Laboratory's main facility is outside Chicago, at 9700 South Cass Avenue, Argonne, Illinois 60439. For information about Argonne and its pioneering science and technology programs, see www.anl.gov.

DOCUMENT AVAILABILITY

Online Access: U.S. Department of Energy (DOE) reports produced after 1991 and a growing number of pre-1991 documents are available free via DOE's SciTech Connect (http://www.osti.gov/scitech/)

Reports not in digital format may be purchased by the public from the National Technical Information Service (NTIS):
U.S. Department of Commerce
National Technical Information Service
5301 Shawnee Rd
Alexandra, VA 22312
www.ntis.gov
Phone: (800) 553-NTIS (6847) or (703) 605-6000
Fax: (703) 605-6900
Email: **orders@ntis.gov**

Reports not in digital format are available to DOE and DOE contractors from the Office of Scientific and Technical Information (OSTI):
U.S. Department of Energy
Office of Scientific and Technical Information
P.O. Box 62
Oak Ridge, TN 37831-0062
www.osti.gov
Phone: (865) 576-8401
Fax: (865) 576-5728
Email: **reports@osti.gov**

Disclaimer
This report was prepared as an account of work sponsored by an agency of the United States Government. Neither the United States Government nor any agency thereof, nor UChicago Argonne, LLC, nor any of their employees or officers, makes any warranty, express or implied, or assumes any legal liability or responsibility for the accuracy, completeness, or usefulness of any information, apparatus, product, or process disclosed, or represents that its use would not infringe privately owned rights. Reference herein to any specific commercial product, process, or service by trade name, trademark, manufacturer, or otherwise, does not necessarily constitute or imply its endorsement, recommendation, or favoring by the United States Government or any agency thereof. The views and opinions of document authors expressed herein do not necessarily state or reflect those of the United States Government or any agency thereof, Argonne National Laboratory, or UChicago Argonne, LLC.

ANL/GTRI/TM-14/6

Out-of-Pile Task 14.5.1: Impact of Mechanical Constraints on Peak Cladding Strain of U-10Mo Monolithic Plate

---

GTRI – Reactor Conversion Program
Out-of-Pile Testing and Codes
Task 14.5.1

Walid Mohamed, Ph.D
Fuels and Materials Modeling Section, Nuclear Engineering Division
Argonne National Laboratory

July, 2014

This work is sponsored by the U.S. Department of Energy,
National Nuclear Security Administration Office of Global Threat Reduction (NA-21)

Out-of-Pile Task 14.5.1: Impact of Mechanical Constraints on Peak Cladding Strain of U-10Mo Monolithic Plate

Walid Mohamed, Ph.D.

Fuels and Materials Modeling Section, Nuclear Engineering Division
Argonne National Laboratory, Bldg. 208 / C145,
9700 S. Cass Avenue, Argonne, IL, 60439

wmohamed@anl.gov

(630)-252-7418 (Work), (919)-802-4651 (cell)

1. Introduction

The effect of external mechanical constraints on the peak cladding strain of U-10Mo monolithic plate was investigated through a FEM based simulation of a 3D model representing L1P756 mini-plate during irradiation.

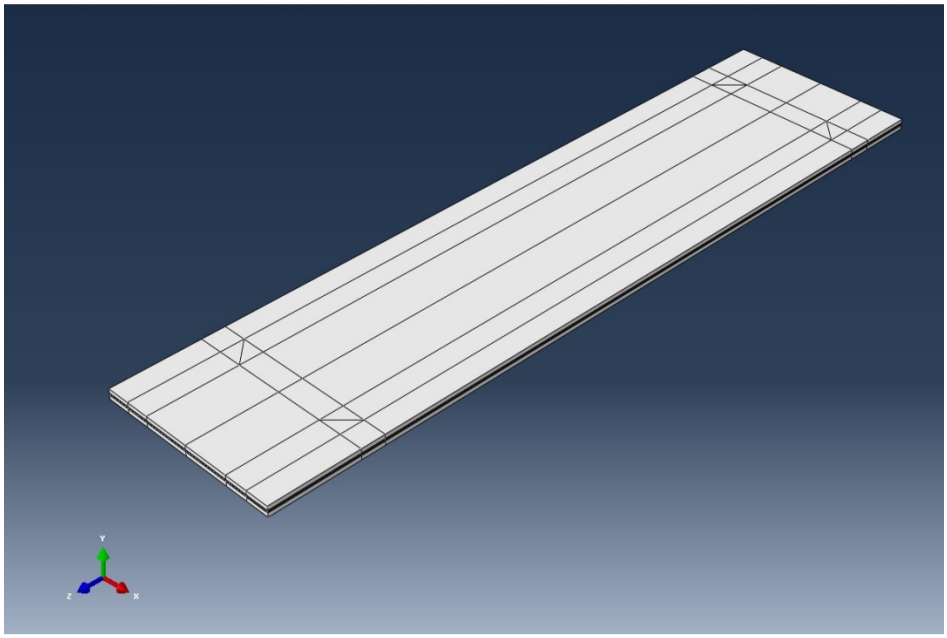

Figure 1 – 3-D model of L1P756 mini-plate

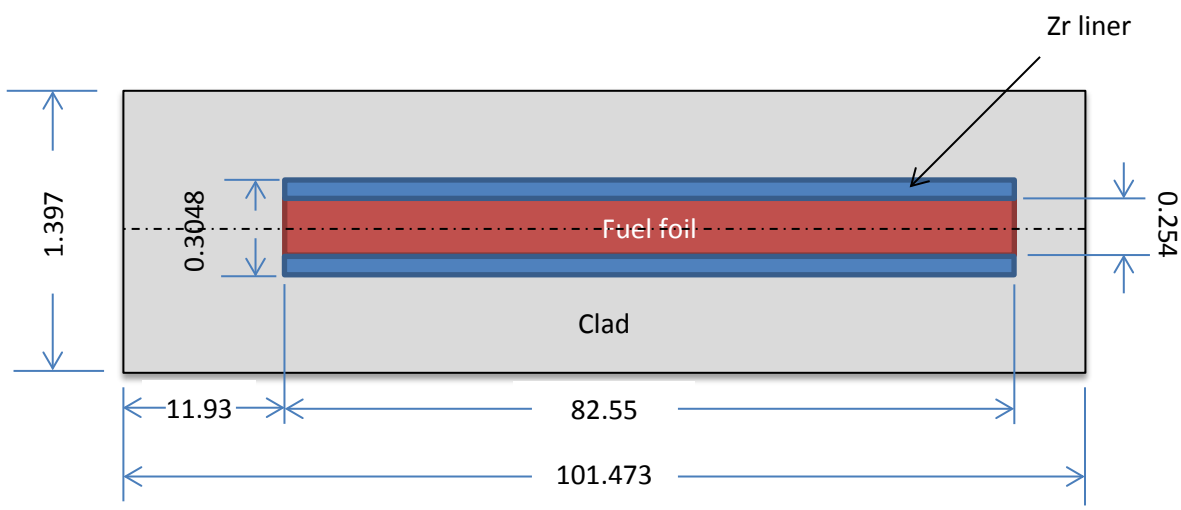

Figure 2 – Schematic of axial section of L1P756 showing the different sections: Clad, fuel foil and Zr liner (dimensions in mm)

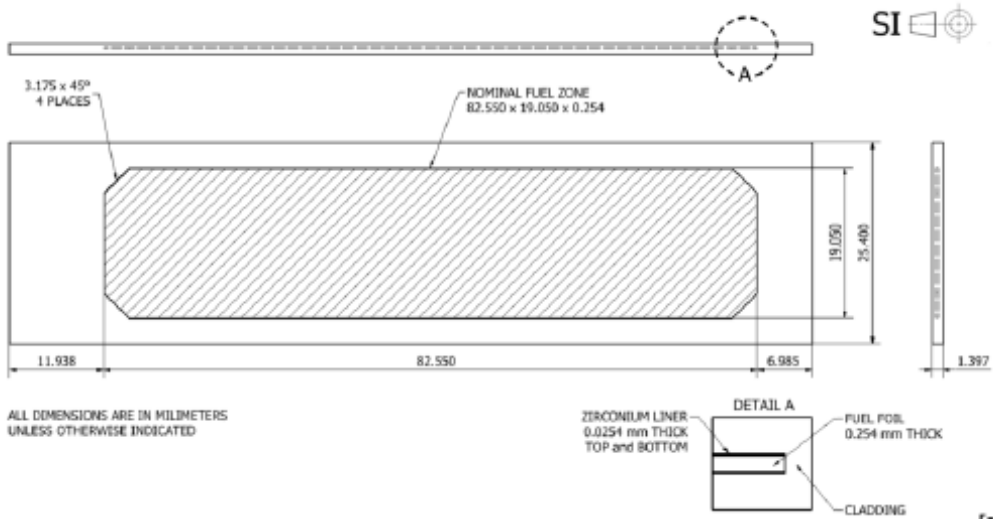

Figure 3 – Dimensions of L1P756 as used in the simulations [1].

2. Simulation and Model Setup

2.1 Simulation model

The irradiation history of L1P756 mini-plate consists of five steps: Startup, ATR cycle 146A, transition from cycle 146A to 146B, ATR cycle 146B, and finally the shutdown (see [1] for details of the irradiation history).

The following are list of the main models which were implemented in the simulations:

(i) model for thermal conductivity degradation of the fuel material [2],
(ii) gaseous swelling model [3],
(iii) irradiation induced creep model [4],
(iv) model for the fuel swelling due to fission products [3]

Details on the coolant channel model are presented in reference [5].

2.2 Simulation approach

Simulation of the irradiation stage of L1P756 via FEM requires implementation of various boundary conditions (B.C.) either to mimic the actual irradiation setup (e.g. the rails holding the mini plate in the reactor core) or to satisfy certain simulation and/ or mathematical requirements (e.g. pseudo rigid body model (PRBM)*, prevent body rotation … etc). Figure 4 shows the different B.Cs. applied in the original 3D model prior to the present study.

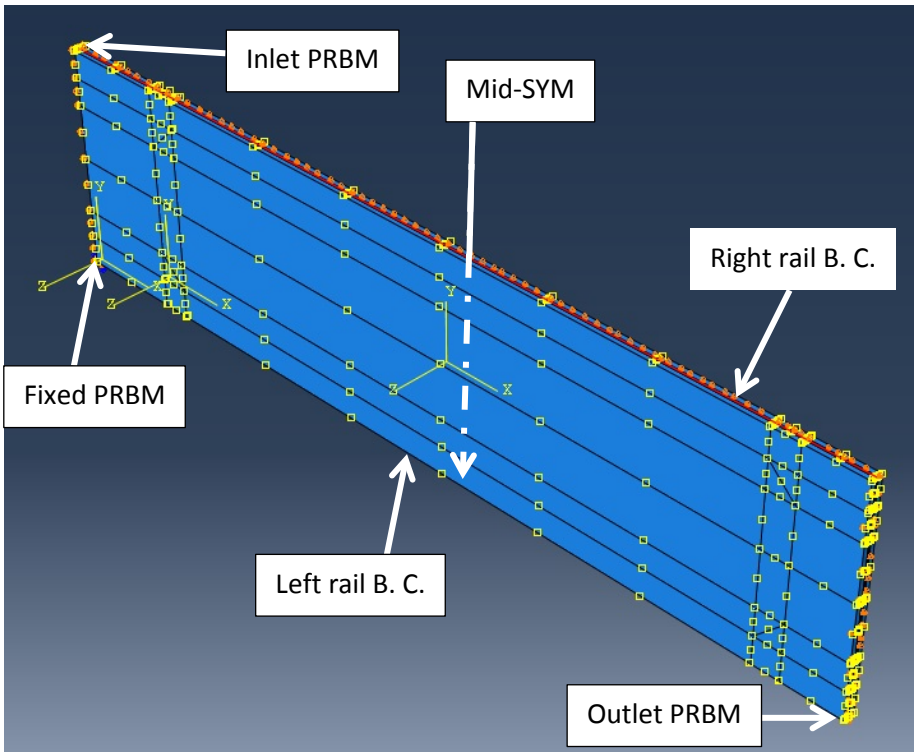

Figure 4: Boundary conditions applied to the original 3D model to simulate irradiation of L1P756 plate

Table 1 – List of boundary conditions and mechanical constraints applied to the 3D model of L1P756

Boundary condition	Description / constrain
Left rail B. C.	Represent the actual constrain on how the plate is being hold in the reactor core: Uy = Uz = 0.0
Right rail B. C.	Represent the actual constrain on how the plate is being hold in the reactor core: Uz = 0.0
Inlet PRBM	Pseudo rigid body model at the coolant inlet side of the plate: Ux=Uz=0.0
Outlet PRBM	Pseudo rigid body model at the coolant inlet side of the plate: Ux=Uz=0.0
Fixed PRBM	Pseudo rigid body model at the left corner of coolant inlet side of the plate to prevent part rotation: Ux= Uy = Uz= Rx = Ry = Rz = 0.0
Mid-SYM	Fixed mid plane of symmetry – no displacement along thickness direction: Uz = 0.0

* Hereby and after will be referred to as PRBM.

According to the boundary conditions listed above and recalling that the major deformation of the plate occurs along the thickness direction (i.e. along the z-axis), the only available surfaces to apply additional mechanical constraints are the two free surfaces at the coolant inlet and outlet sides of the monolithic plates as shown in Figure 5.

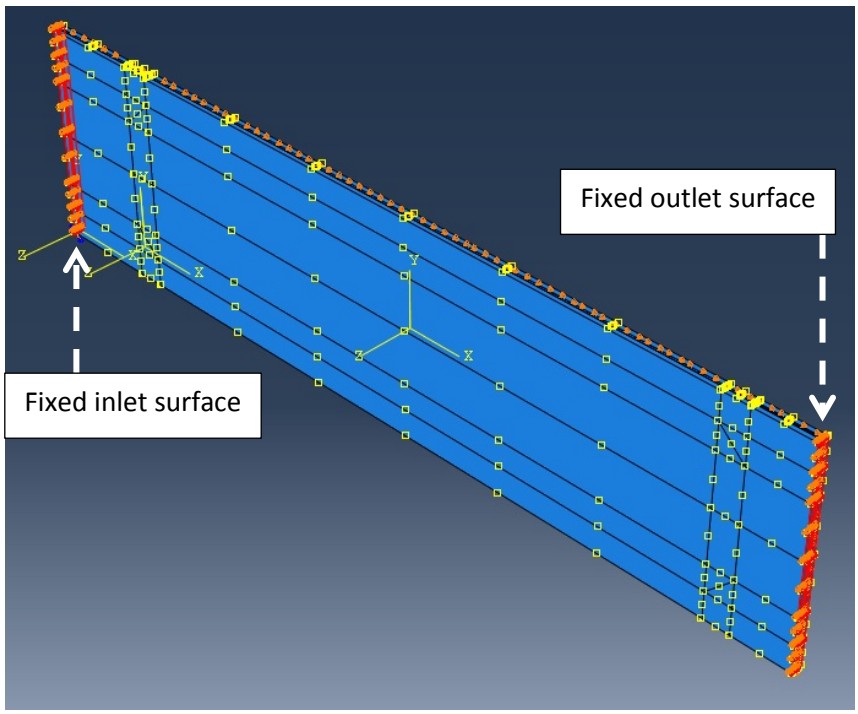

Figure 5: Free surfaces at coolant inlet and outlet sides highlighted in red where external mechanical will be applied

The applied mechanical constraints on the free surfaces imply that the displacement deformation of these surfaces along the coolant flow direction (i.e. along the x-direction) equals zero (Ux= 0.0).

3. Results and Discussion

3.1 Strain profile of cladding with mechanical constraints

The cladding strain profiles during the different stages of irradiation (start up, cycle 146A, transition between 146A and 146B, cycle 146B, and shutdown) were tracked with mechanical constraints applied and compared to the corresponding profiles of the original model. The strain was described in terms of the equivalent plastic strain to consider any permanent strain/ deformation induced by the mechanical constraints.

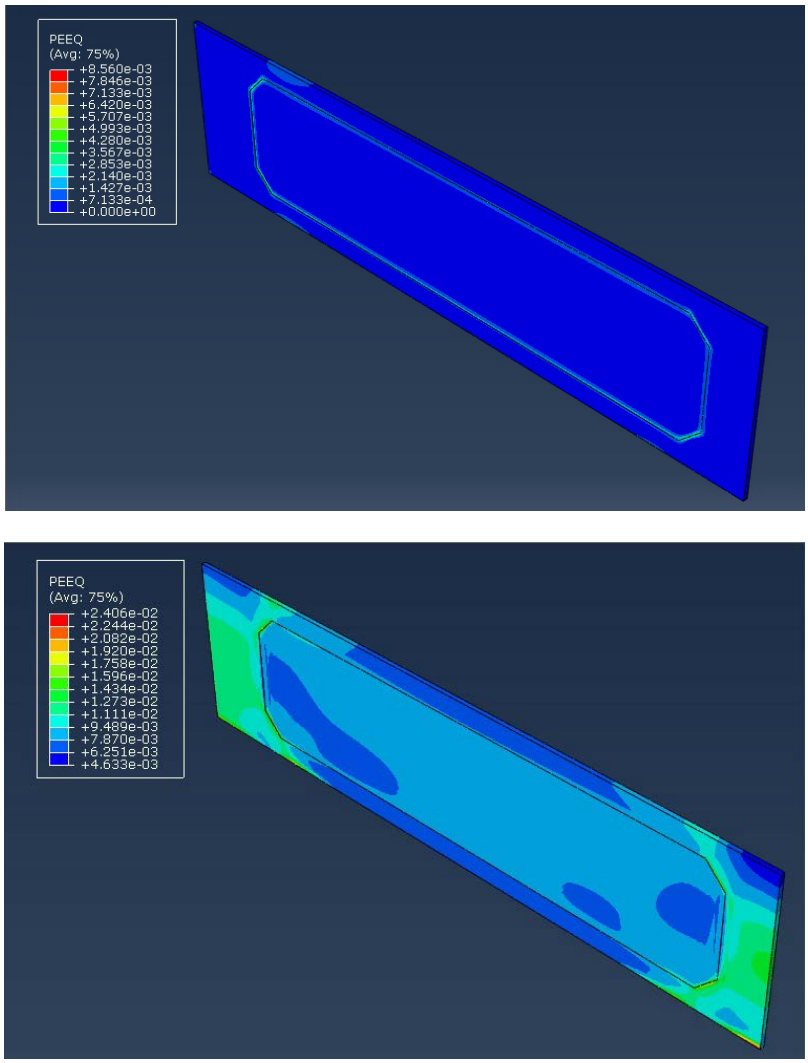

Figure 6: Equivalent plastic strain in cladding at the end of startup up stage in the original 3D model of the plate (top) and with the coolant inlet and outlet surfaces mechanically constrained (bottom).

According to the strain profiles shown in Figure 6, the applied mechanical constraints at the coolant inlet and outlet sides caused the peak cladding strain to increase from 8.56E-03 to 2.41E-02 (difference ~ 0.0155) at the end of startup stage. Although the peak cladding strain is apparently localized in the vicinity of the applied mechanical constraints, the overall equivalent plastic strain in higher everywhere else compared to the corresponding original model.

By the end of irradiation (i.e. shutdown), the difference in maximum equivalent plastic strain between the original 3D model and the corresponding one with mechanical constraints dropped from 0.0155 to 0.0143 (~ 9% less) as shown in the Figure 7.

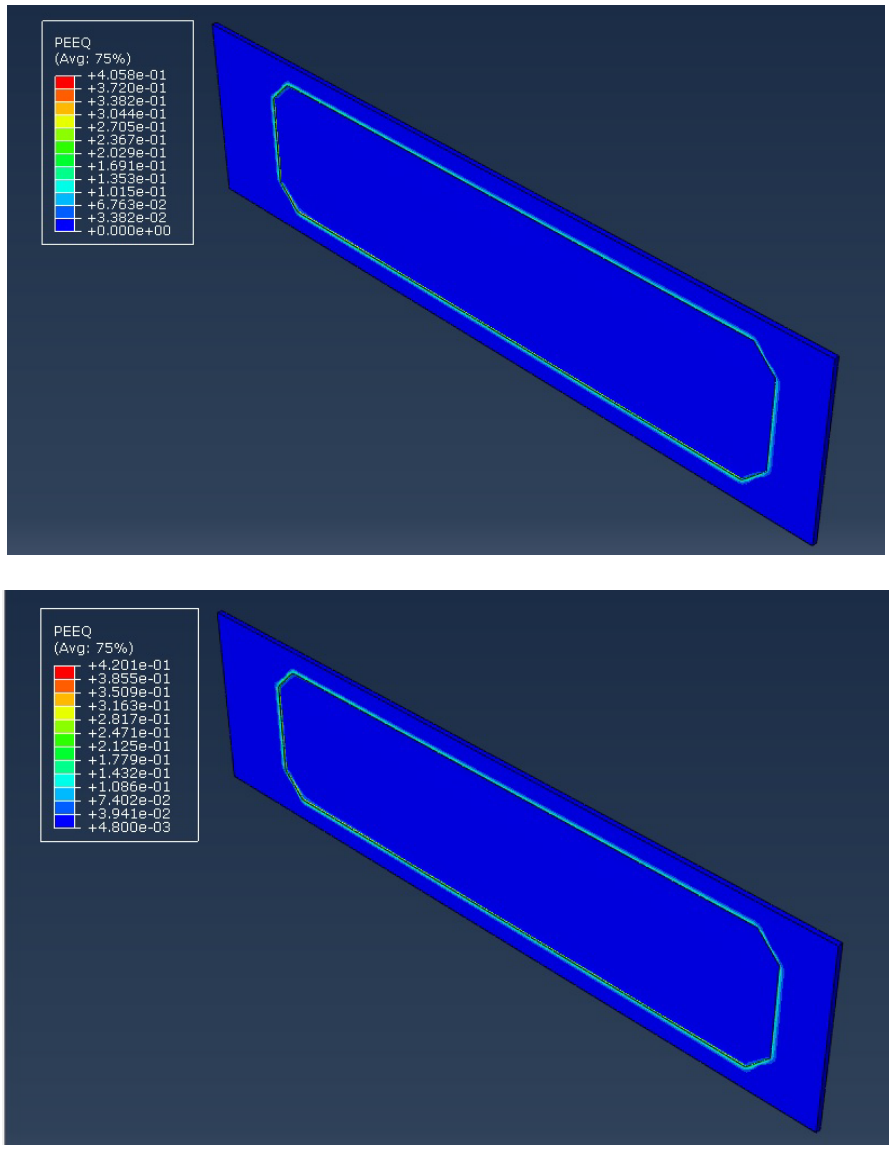

Figure 7: Equivalent plastic strain (mm/mm) in cladding at the end of shutdown stage in the original 3D model of the plate (top) and with the coolant inlet and outlet surfaces mechanically constrained (bottom).

For further analysis, the variation of the peak cladding of the two models over the different irradiations cycles as well as the difference in peak cladding strains are shown in Figure 8 and 9 respectively.

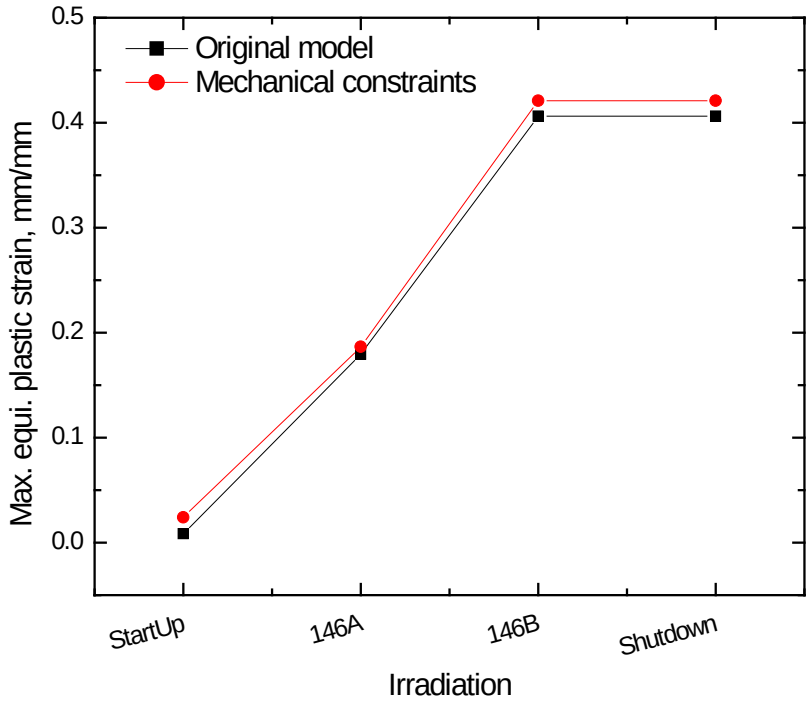

Figure 8: Variation of peak clad strain over the irradiation stage of L1P756 monolithic plate in RERTR-12

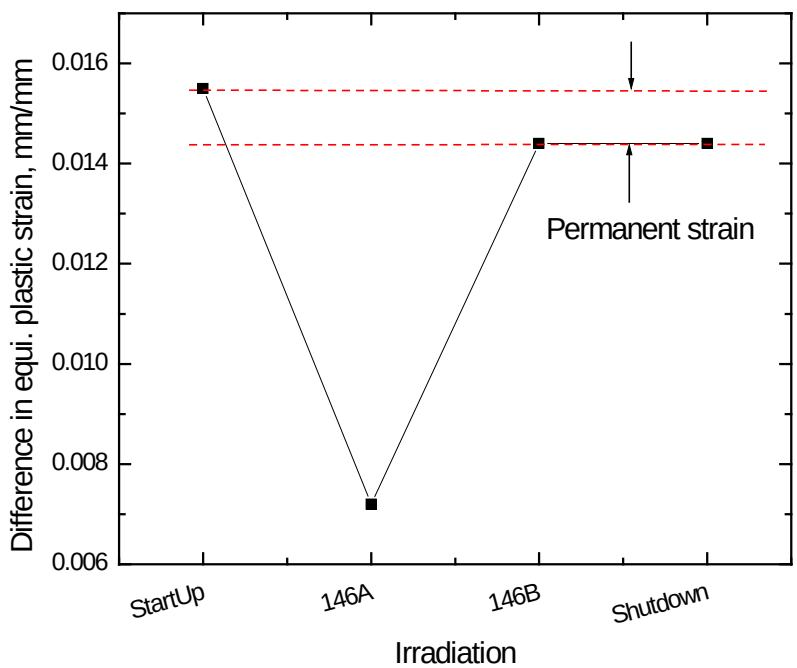

Figure 9: Difference in peak cladding strain between the two models over the irradiation stage

The data shown in Figure 8 indicates that the difference in peak cladding strain between the original model and the mechanically constrained one is highest at the beginning of irradiation and becomes minimum just by the end of irradiation cycle 146A. Finally, it saturates to be about 0.0143 till the end of irradiation.

Moreover, the variation in the difference in peak cladding strain as shown in Figure 9 indicates that the initial cladding strain induced by the mechanical constrained was “partially” relived (about 8% less) by the end of the irradiation cycle 146A.

Obviously, the mechanical constrained applied in this case resulted in a permanent plastic strain in the cladding of about 0.0143 which is about 3.5% of the peak cladding strain computed for the original model (maximum equivalent plastic strain of 0.4058).

3.2 Asymmetric mechanical constraints

Due to the asymmetrical geometry of the L1P754 monolithic plate along the axial direction (i.e. the coolant flow direction), other states of mechanical constraints were investigated by preventing axial displacement at the coolant inlet and outlet sides separately.

With mechanical constraints applied to the coolant inlet side, minimal change in the peak cladding strain was observed when compared to the original model as shown in Figure 10.

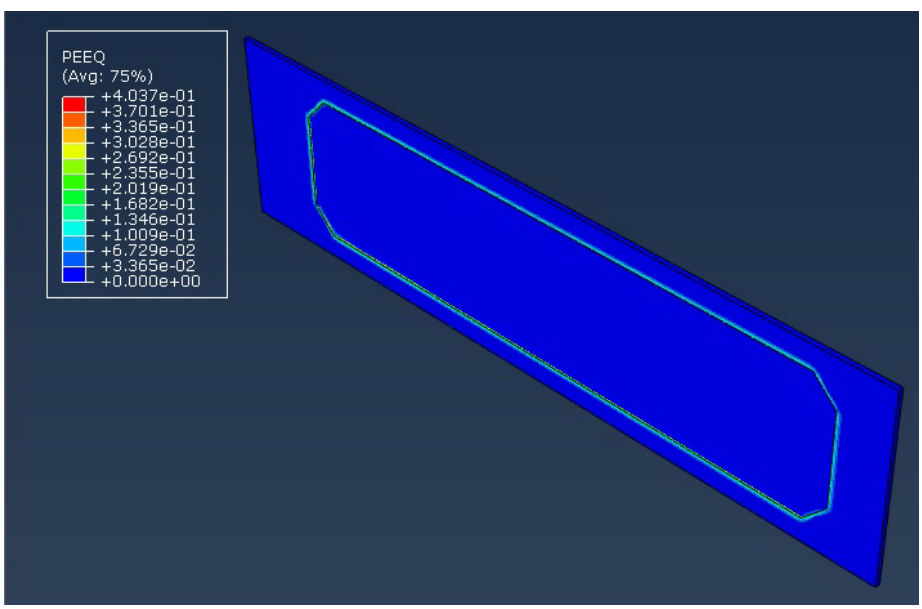

Figure 10: Equivalent plastic strain in cladding at shutdown with mechanical constraints applied only at the coolant inlet side showing peak cladding strain 0.4037.

When mechanical constraint was attempted at the coolant outlet side, the numerical solution encountered severe convergence problem due to excess deformation/ strain at large number of nodes and solution convergence was judged unlikely.

Recalling the geometry of the monolithic plate under investigation (see Figure 2), the cladding material content is higher toward the coolant inlet side compared to the coolant outlet side which explains the capability of the model to accommodate the excess strain induced by the mechanical constraints when applied to the inlet side. Similarly, the failure to accommodate the plastic strain induced by the mechanical constraints being applied at the coolant outlet side is attributed to the limited cladding material content in this region.

3.3 Relaxation of boundary conditions

As mentioned earlier in this reports, the boundary conditions applied to the L1P756 model are either to mimic actual mechanical state (fixtures, constraints … etc) of the plate or to satisfy physical and/ or mathematical considerations (rigid body, rotation … etc). In this subsection, the corresponding strain field of cladding following relaxation of some of the B.Cs listed in Table -1.

When the three PRBM B.C. were suppressed, an increase of about 1.4% in peak cladding equivalent plastic strain was observed while suppression of the mid-symmetry plane B.C. caused less than 0.5% increase in the peak cladding strain.

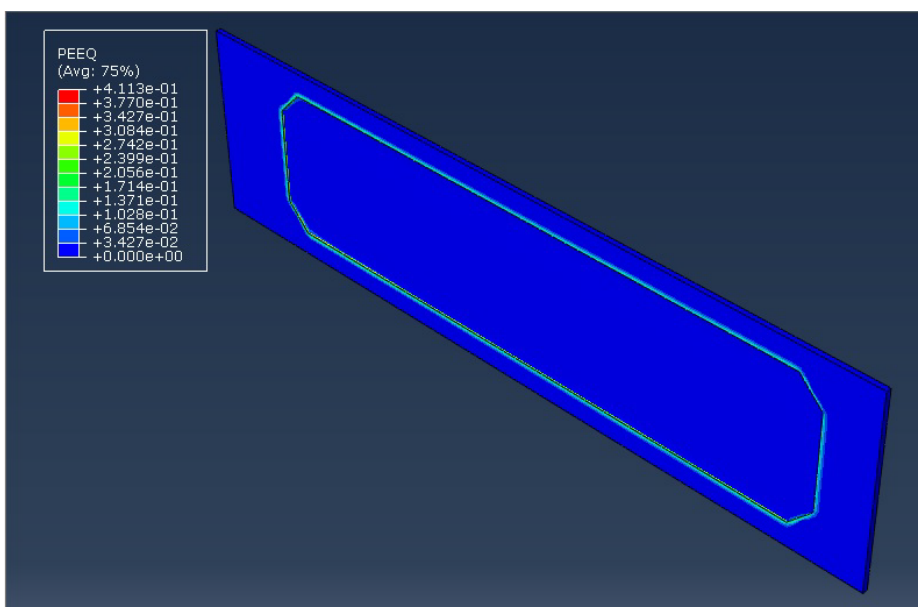

Figure 11: Equivalent plastic strain in cladding at shutdown with all PRBM boundary conditions being suppressed

Compared to the 3.5% increase in peak cladding strain with mechanical constraints, it is worthwhile to consider the implementation of PRBM boundary conditions to avoid over estimating the simulated peak cladding strain.

4. Summary

The impact of mechanical constraints on the peak cladding strain was investigated by simulating different states of mechanical constraints on the 3-D model of L1P756 monolithic plate. With symmetric mechanical constraints applied at the coolant inlet and outlet sides, an early increase in peak cladding strain was observed by the end of irradiation cycle 146A followed by partial strain relief during the rest of the irradiation course. By the end of irradiation, the cladding section accumulated permanent plastic strain of about 0.0143 which represents 3.5% of the peak cladding strain without any mechanical constraints applied.

The influence of the symmetry of the mechanical constraints was examined by applying constraints separately at the coolant inlet and outlet sides. With the coolant inlet side being constrained, minimal change in peak cladding strain was observed which indicates that the major contribution to the increase in peak cladding strain with symmetric mechanical constraints comes from the constraint applied at the coolant outlet side. This observation was confirmed by the failure of solution convergence when mechanical constraint was applied solely at the coolant outlet side due to severe deformation at large number of nodes. It is suggested that the observed mechanical response of the L1P756 monolithic plate to the asymmetric mechanical is mainly due to the asymmetric cladding material content along the axial direction of the plate (i.e. along the coolant flow direction). Thus, it is worthwhile to notice that the mechanical response of monolithic plates to mechanical constraints is highly dependent on the applied constraints as well as the plate geometry itself.

References

[1] D. M. Perez *et al*., "RERTR-12 Insertion 1 Irradiation Summary", INL/EXT-11-24101, September 2012.

[2] S.L. Hayes, G.L. Hofman, M.K. Meyer, and J. Rest, "Modeling of High Density U-Mo Dispersion Fuel Plate performance", 24th International Meeting on RERTR, San Carlos de Bariloche, Argentina, 2002.

[3] Y.S. Kim and G.L. Hofman, "Fission Product Induced Swelling of U-Mo Alloy Fuel", Journal of Nuclear Materials, Vol. 419, pp291-301, 2011.

[4] Y.S. Kim *et al*., "Fission Induced Swelling and Creep of U-Mo Alloy Fuel", Journal of Nuclear Materials, vol. 437, pp 37-46, 2013.

[5] Hakan Ozaltun, Robert M. Allen, You Sung Han, "Effect of the Zirconium Liner Thickness on the Stress-Strain Characteristics of U10Mo Alloy Based Monolithic Mini-Plates", Proceedings of the ASME 2013, IMECE2013, Nov. 13-21, 2013, San Diego, CA, USA.

Nuclear Engineering Division
Argonne National Laboratory
9700 South Cass Avenue, Bldg. 208
Argonne, IL 60439

www.anl.gov

Argonne National Laboratory is a U.S. Department of Energy
laboratory managed by UChicago Argonne, LLC